Argonne v-18 nucleon-nucleon potential: different radial components

Ref: Wiringa, Stoks & Schiavilla, Phys. Rev. C 51, 38 (1995)

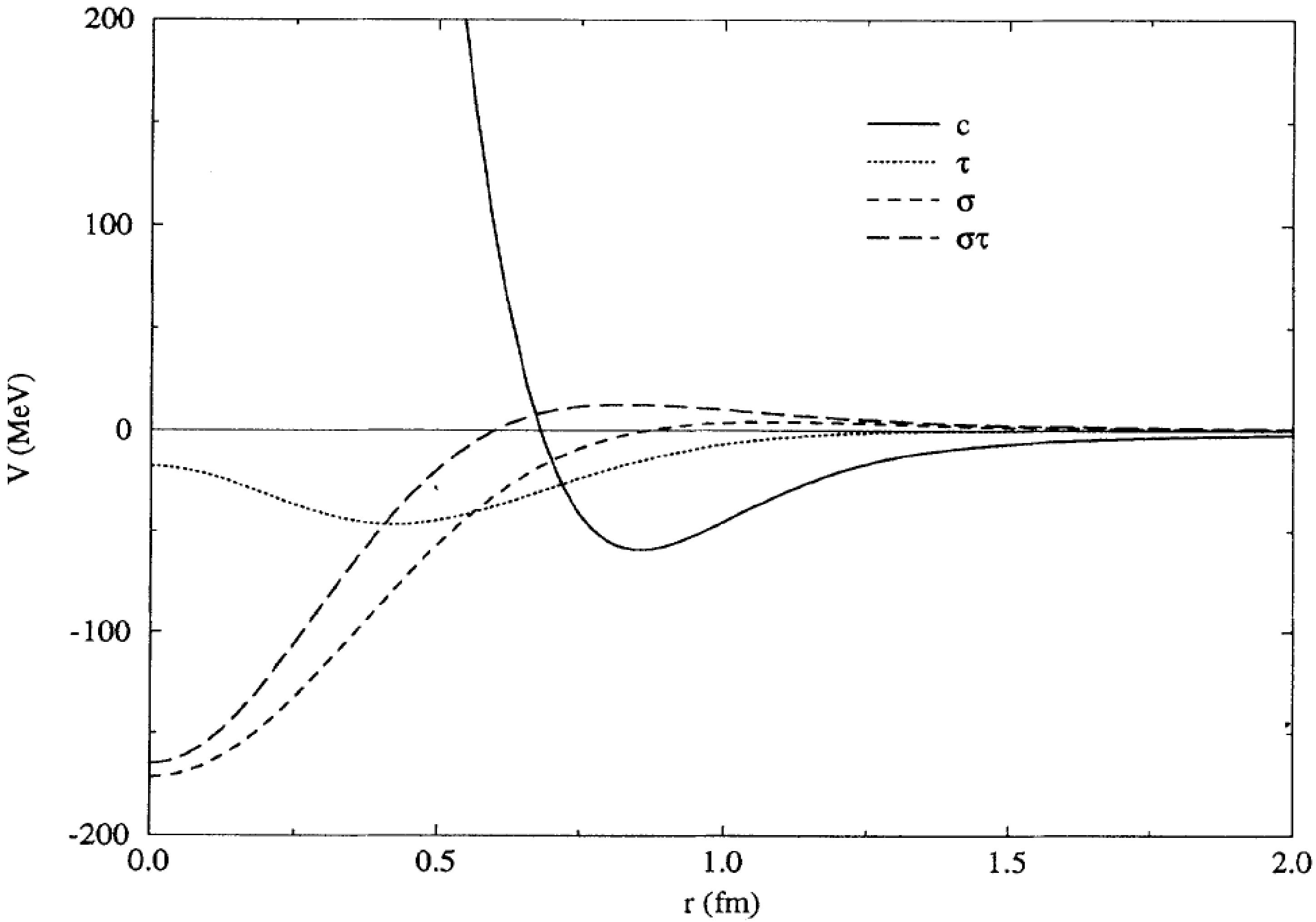

FIG. 6. Central, isospin, spin, and spin-isospin components of the potential. The central potential has a peak value of 2031 MeV at $r = 0$.

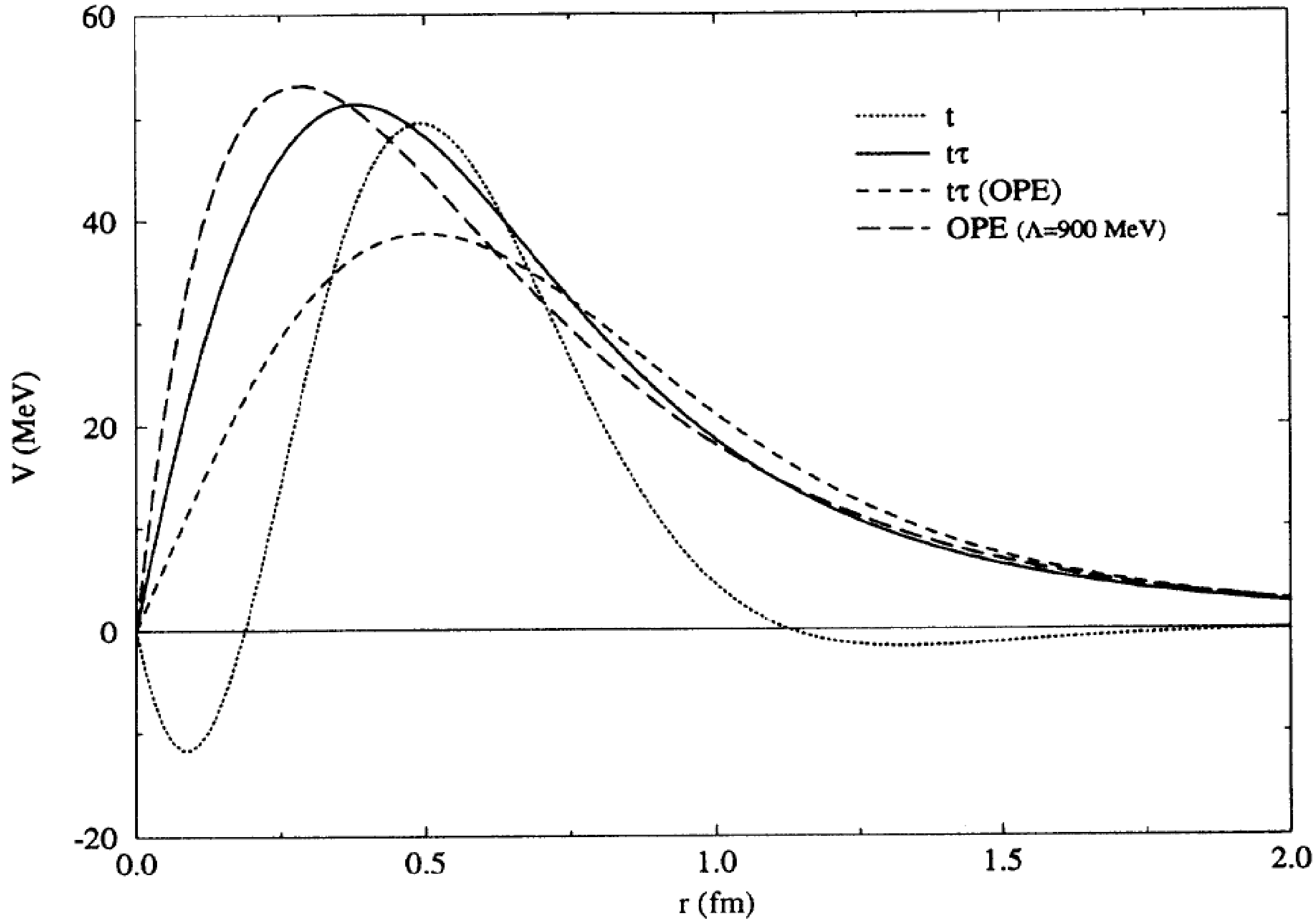

FIG. 7. Tensor and tensor-isospin parts of the potential. Also shown are the OPE contribution to the tensor-isospin potential, and for comparison an OPE potential with a monopole form factor containing a 900 MeV cutoff mass.

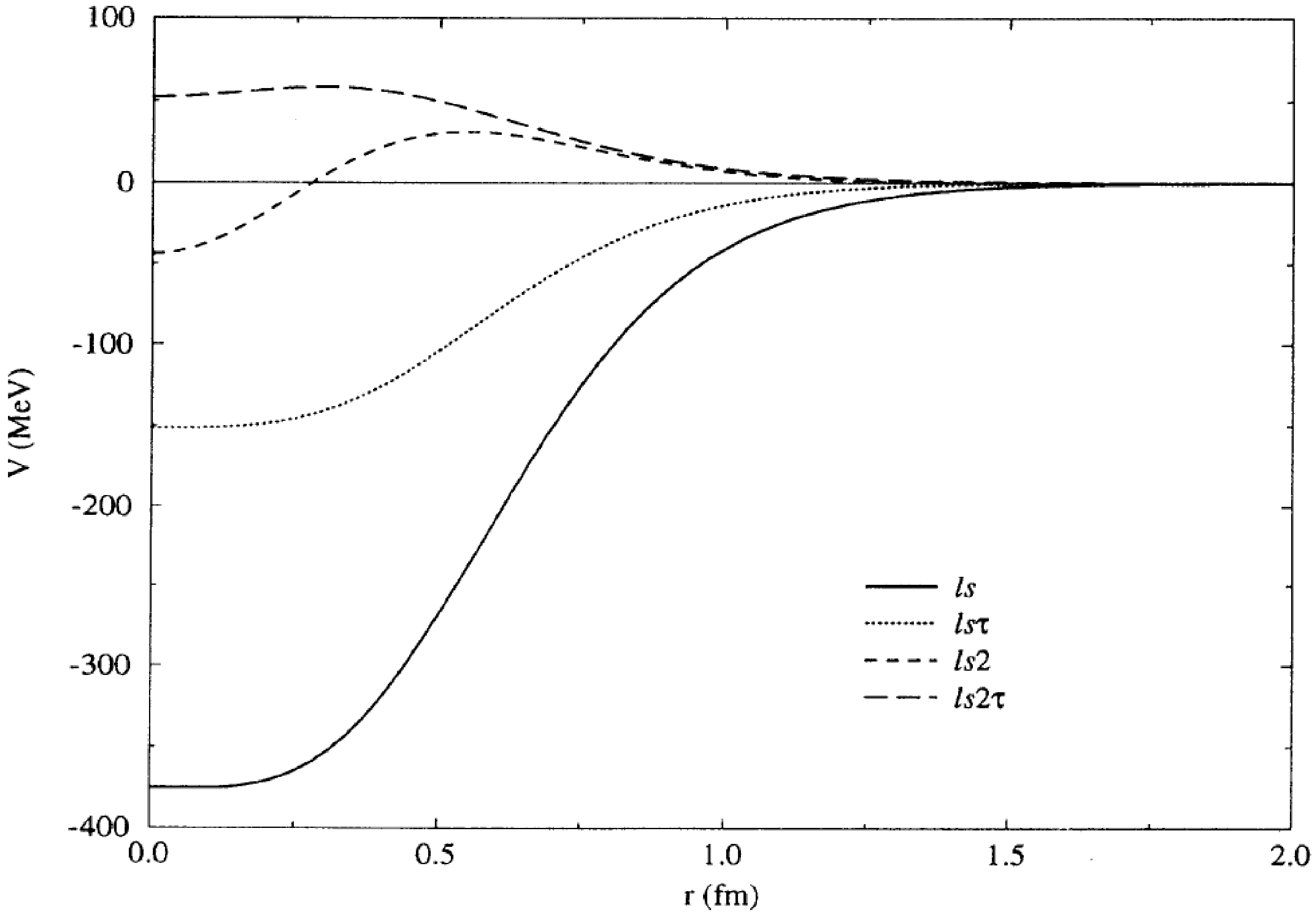

FIG. 8. Spin-orbit and quadratic spin-orbit components of the potential.

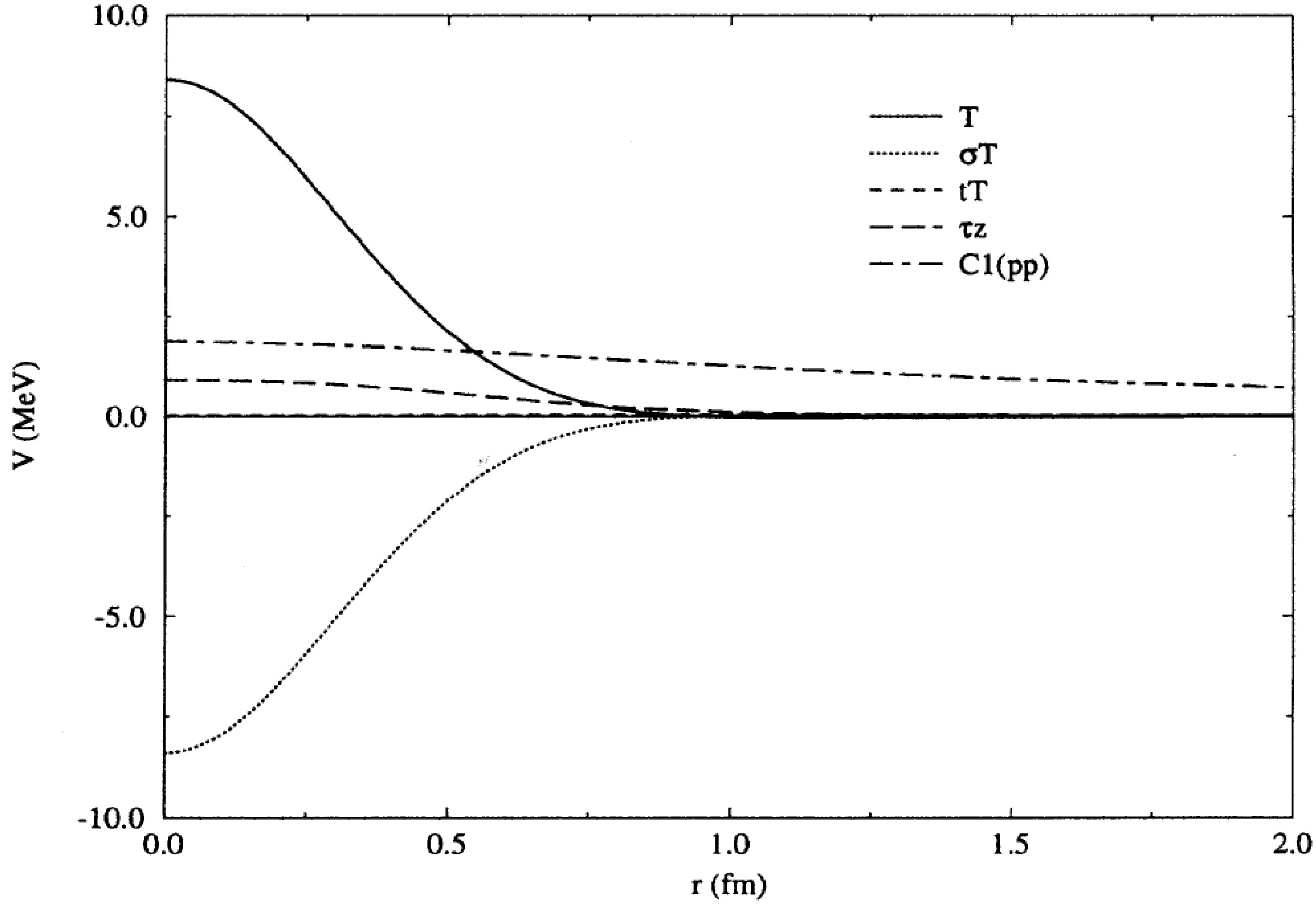

FIG. 10. Charge-dependent and charge-asymmetric components of the potential. Also shown for comparison is the Coulomb potential, $V_{C1}(pp)$.

Derive N-N interaction potentials from meson exchange theories

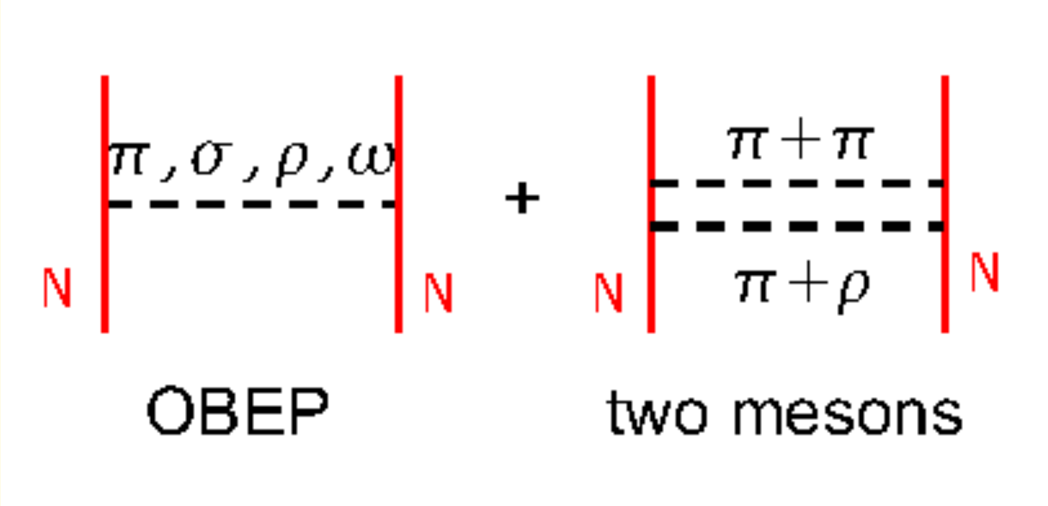

Most important: 1-pion exchange potential (OPEP) contributes to spin-isospin (σ τ) and tensor-isospin (t τ) components of Argonne v-18 potential

Experimental p-p and n-p differential cross sections

Ref: W.N. Hess, Rev. Mod. Phys. 30, 368 (1958)

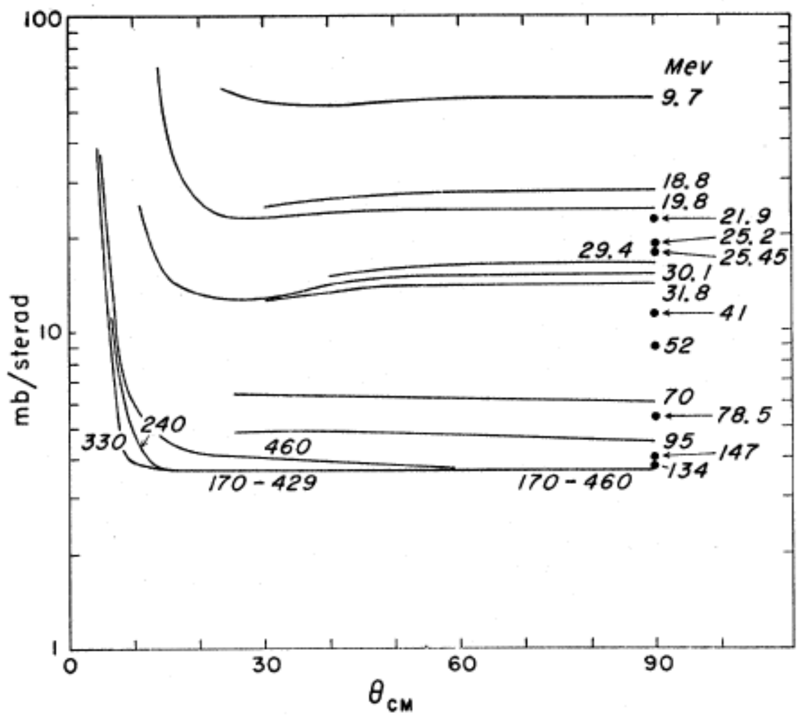

FIG. 6. Experimental values of the differential proton-proton cross section at various energies up to 500 Mev.

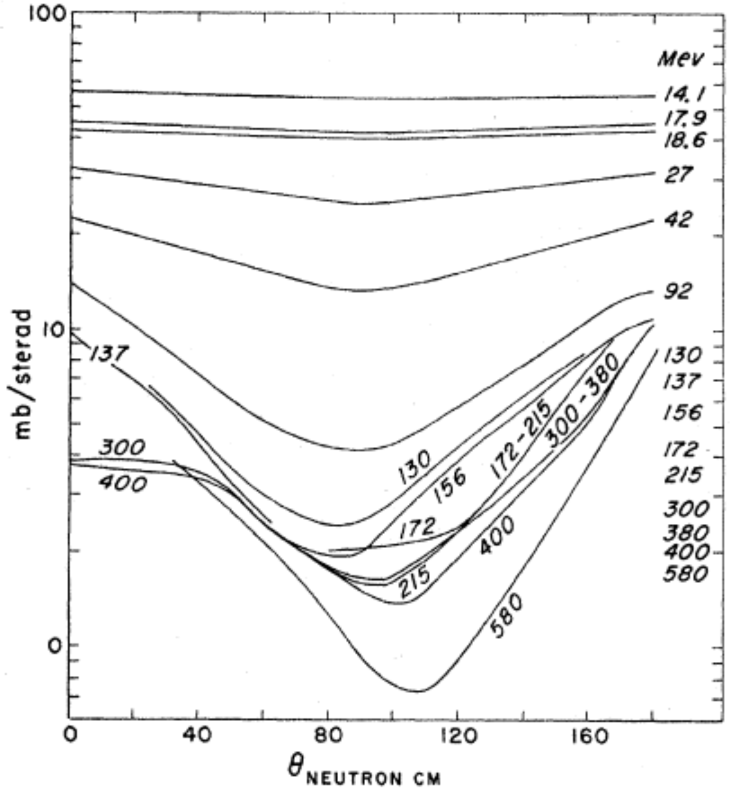

FIG. 5. Experimental values of the differential neutron-proton cross section at various energies.

N-N quantum states

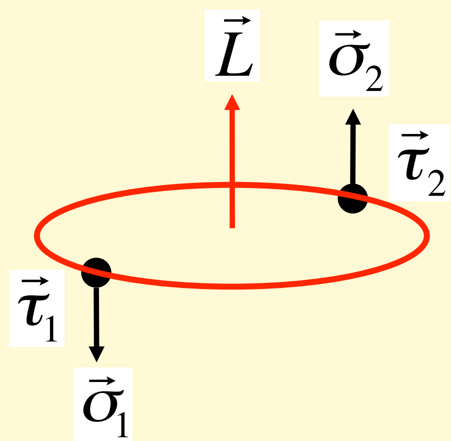

$\vec{L} = \vec{r} \times \vec{p}$ — orbital ang. momentum

$\vec{S} = \frac{\hbar}{2}\left(\vec{\sigma}_1 + \vec{\sigma}_2\right)$ — spin of N-N pair

$\vec{J} = \vec{L} + \vec{S}$ — total ang. momentum

$\vec{T} = \frac{1}{2}\left(\vec{\tau}_1 + \vec{\tau}_2\right)$ — isospin of N-N pair

Spectroscopic notation: $^{(2S+1)}L_J$ use S,P,D,... for L=0,1,2,...

N-N state vector: $\left|\Psi(1,2)\right\rangle = \left|LS;JM_J\right\rangle \otimes \left|T,T_z\right\rangle$

Free N-N interaction: Reid soft-core potential (1968)
for some of the reaction channels

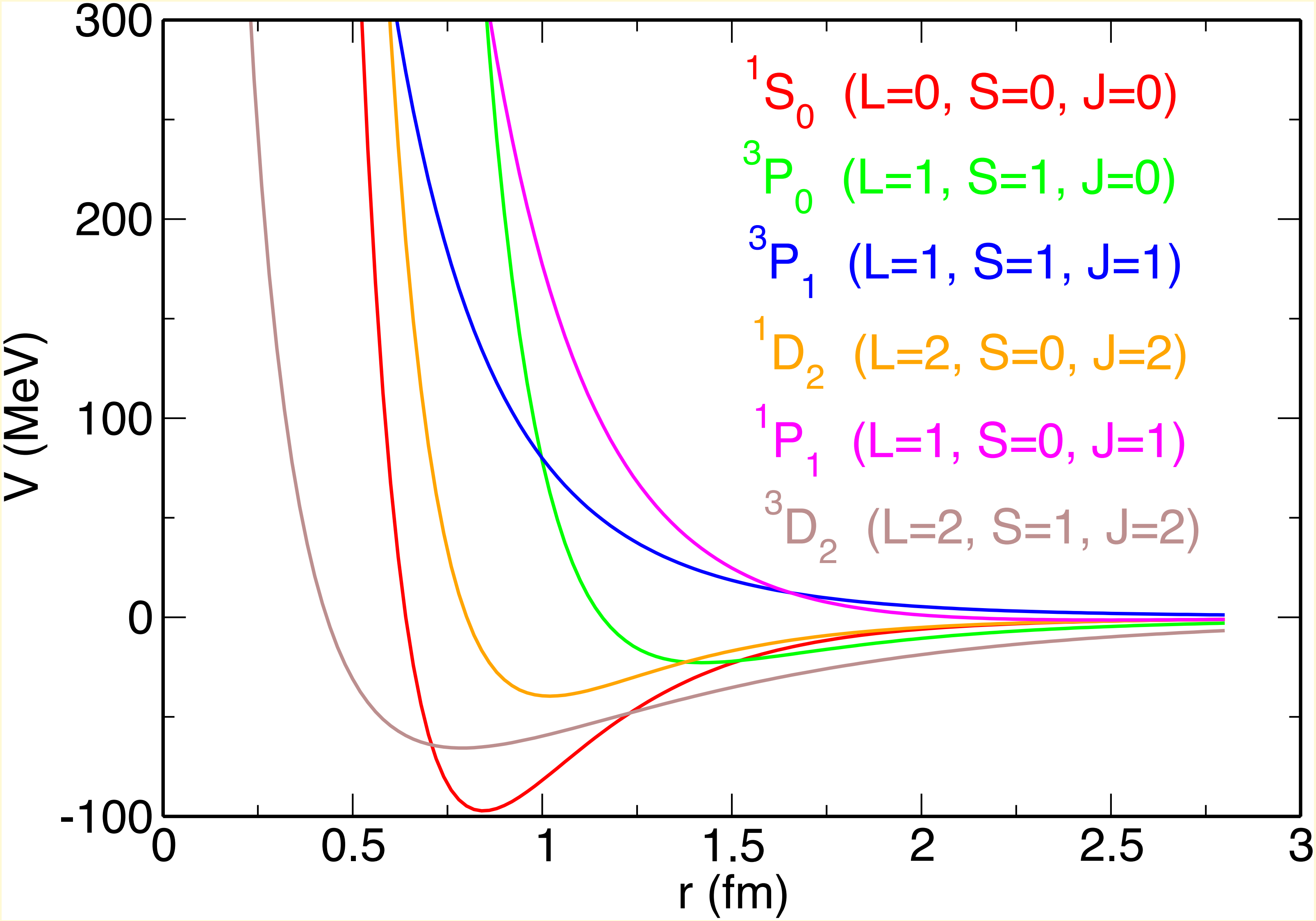

Phase shifts for “Nijmegen potentials” based on recent N-N scattering data
(E_{lab} = 0 - 400 MeV)

Ref: Stoks et al., Phys. Rev. C49 (1994) 2950

Phase shifts for Argonne v-18 potential and comparison with Nijmegen N-N data analysis

Ref: Wiringa, Stoks & Schiavilla, Phys. Rev. C 51, 38 (1995)

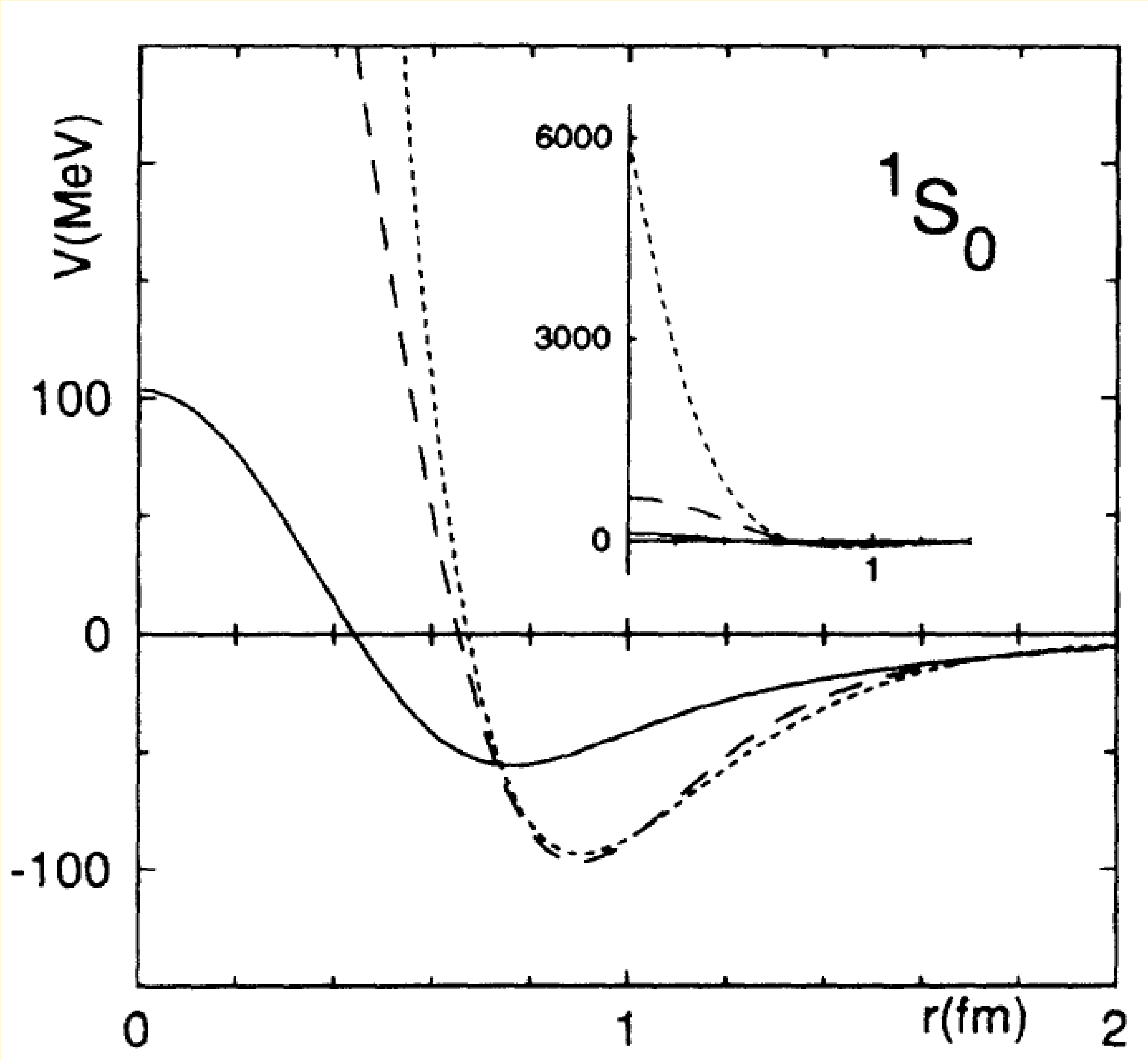

Nijmegen N-N potentials (1994)

solid line: Nijm 1 (non-local)

dashed line: Nijm 2 (local)

dotted line: Reid 93

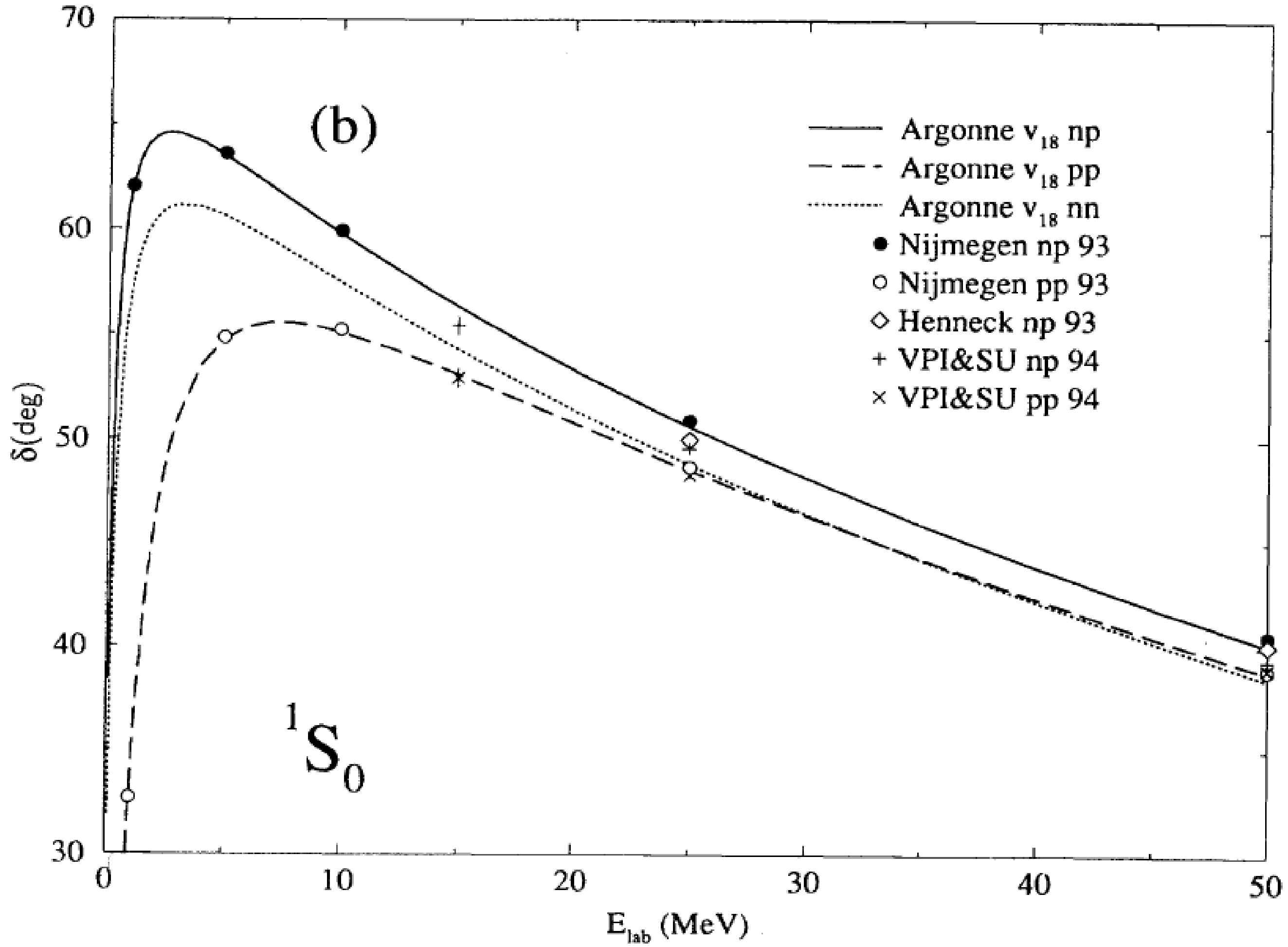

FIG. 2. Phase shifts in the $^1S_0$ channel for *np*, *nn*, and *pp* scattering, compared to various partial-wave phase-shift analyses.

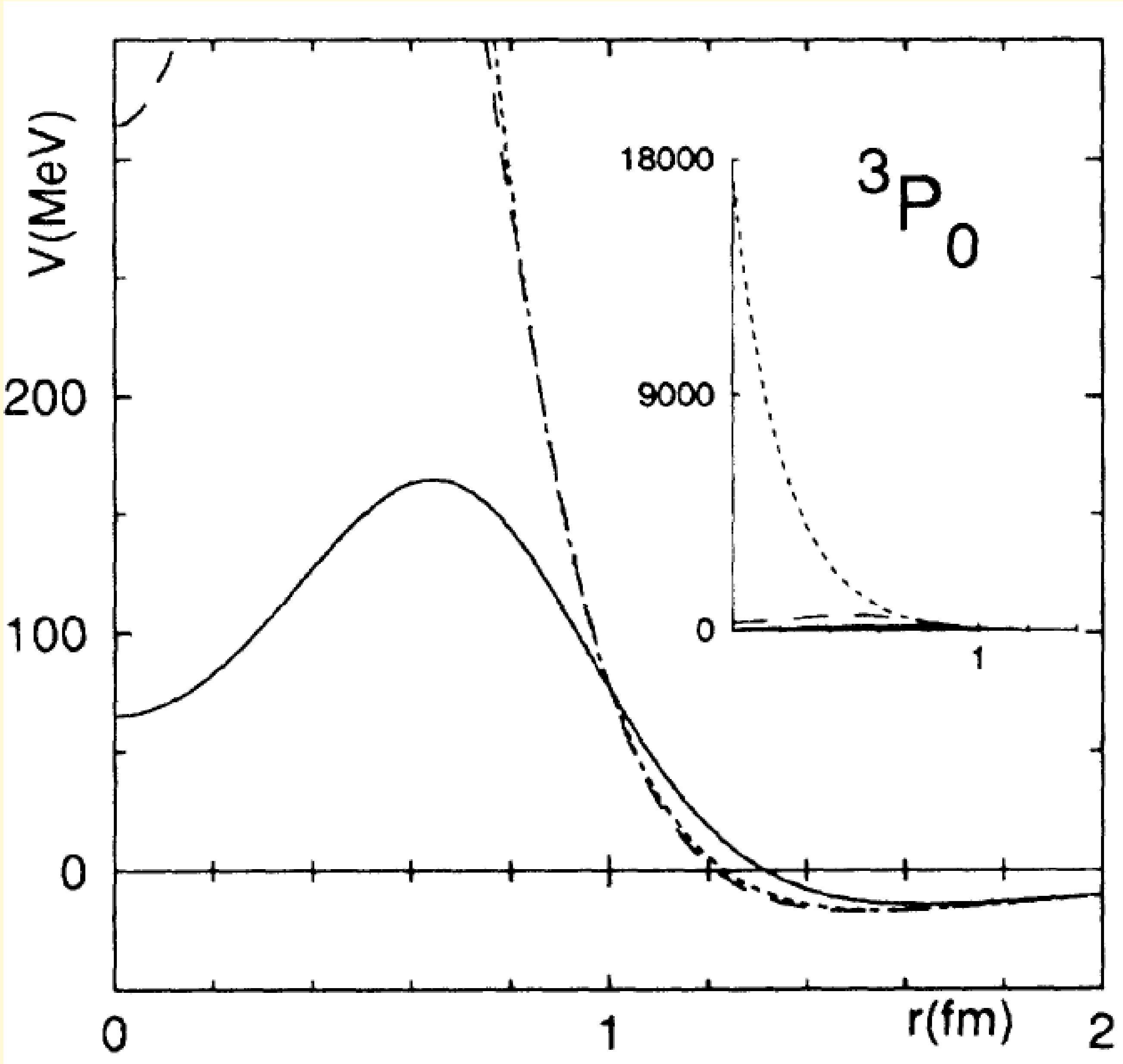

Nijmegen N-N potentials (1994)

solid line: Nijm 1
(non-local)

dashed line: Nijm 2
(local)

dotted line: Reid 93

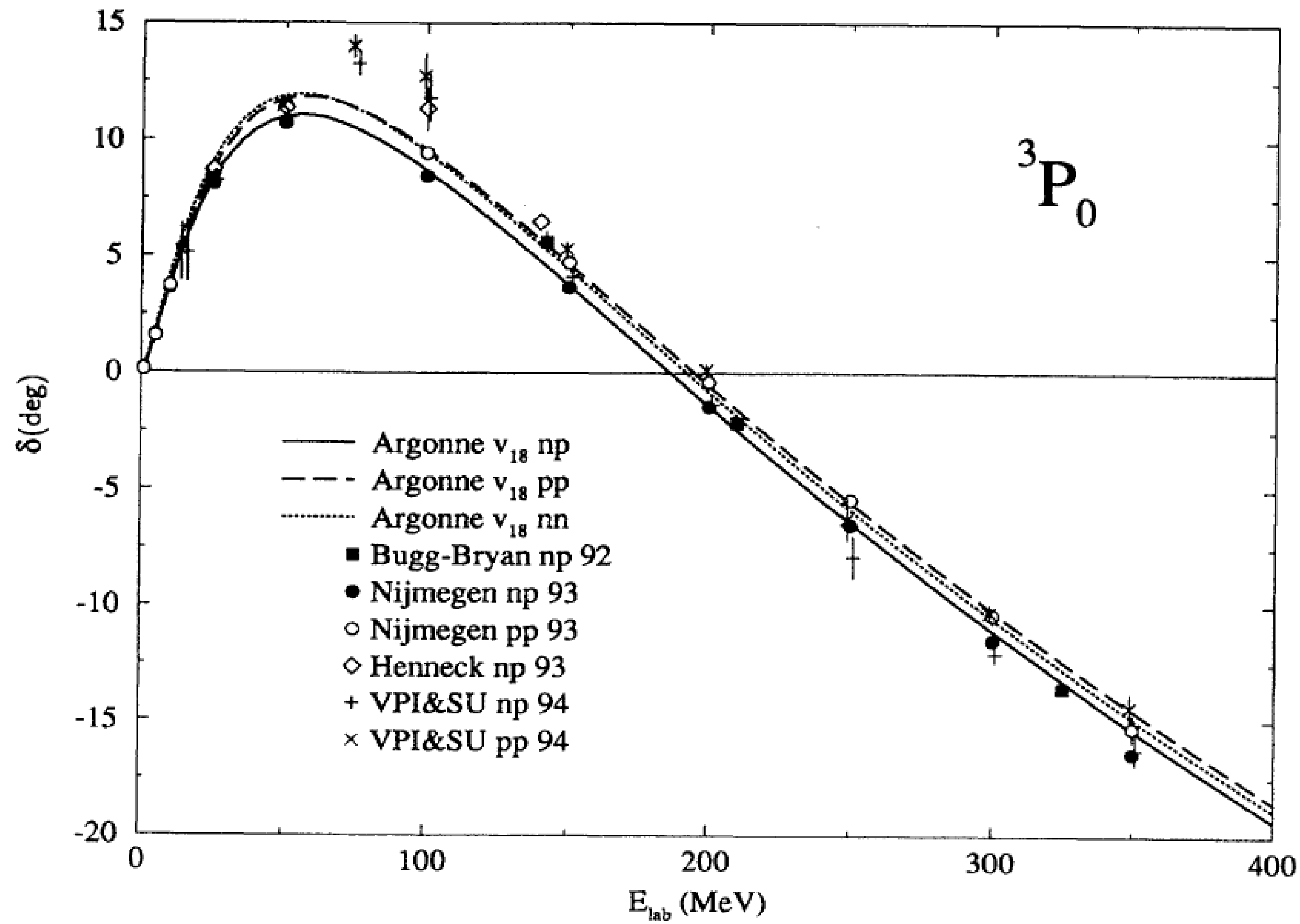

FIG. 3. Phase shifts in the $^3P_0$ channel for *np*, *nn*, and *pp* scattering, compared to various partial-wave phase-shift analyses.

Nijmegen phase shift analysis of all p-p scattering data below 350 MeV

Ref: J.R. Bergervoet et al., Phys. Rev. C 41, 1435 (1990)

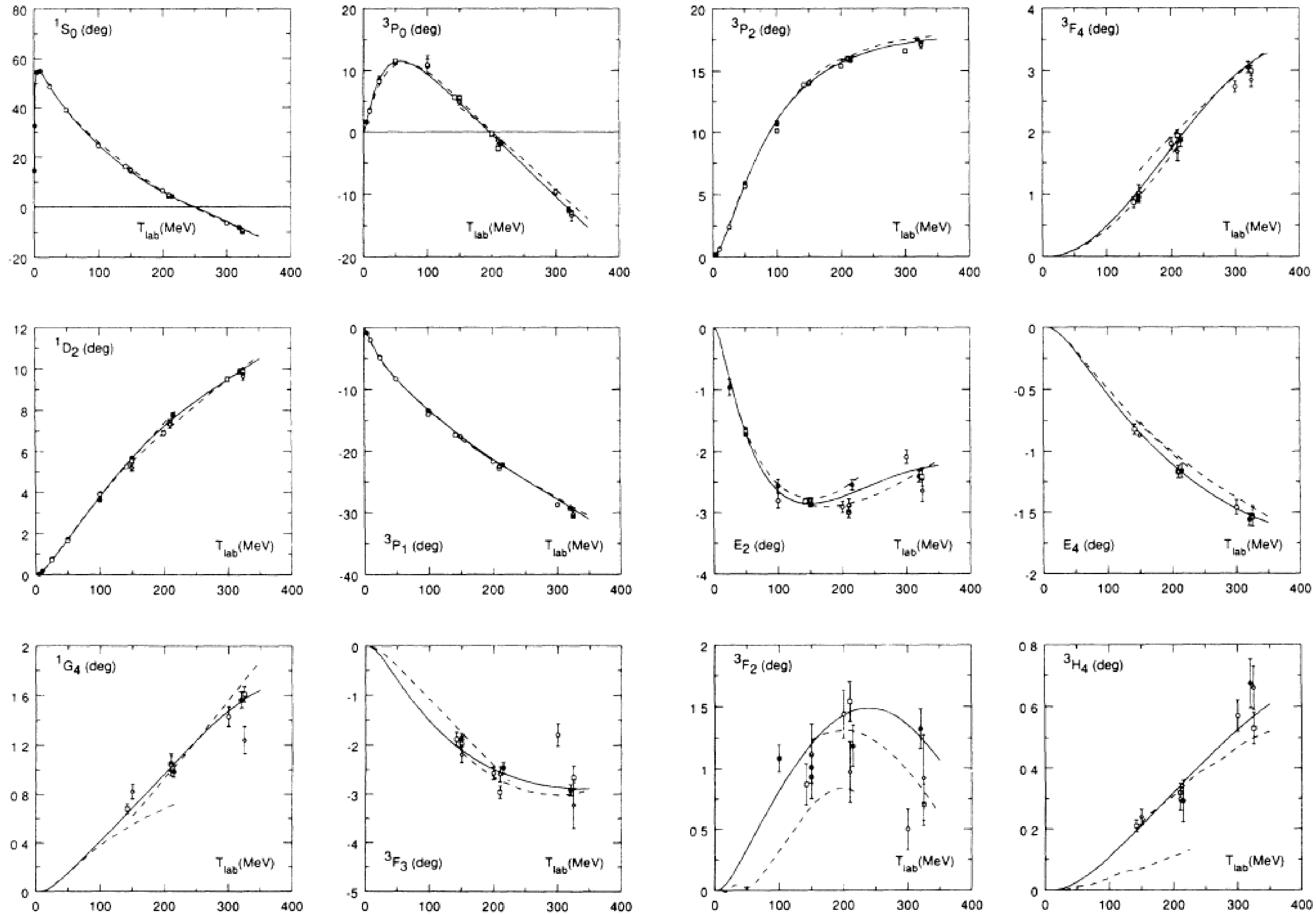

FIG. 1. Phase shifts in degrees vs T_{lab} in MeV. Errors are shown only if they are large enough to be plotted. Solid line: multienergy analysis; dashed line: Bystricky *et al.* (Ref. 6). ●: single-energy analysis; ○: Arndt *et al.* (Ref. 7); □: Dubois *et al.* (Ref. 18); ◇: Bugg *et al.* (Ref. 19).